Chapter 1

NUMERICAL SIMULATION OF HIGH MACH NUMBER ASTROPHYSICAL JETS

Carl L. Gardner
Department of Mathematics and Statistics, Arizona State University, Tempe AZ 85287

Youngsoo Ha
Division of Applied Mathematics, Korean Advanced Institute of Science and Technology, Taejon, South Korea 305-701

J. Jeff Hester
Department of Physics and Astronomy, Arizona State University, Tempe AZ 85287

John E. Krist
Jet Propulsion Laboratory, Pasadena CA 91109

Chi-Wang Shu
Division of Applied Mathematics, Brown University, Providence RI 02912

Karl R. Stapelfeldt
Jet Propulsion Laboratory, Pasadena CA 91109

Abstract Computational fluid dynamics simulations using the WENO-LF method are applied to high Mach number nonrelativistic astrophysical jets, including the effects of radiative cooling. Our numerical methods have allowed us to simulate astrophysical jets at much higher Mach numbers than have been attained (Mach 20) in the literature. Mach 80 simulations of the HH 1-2 astrophysical jets and the XZ Tauri proto-jet are presented.

1. Introduction

A new wealth of detail in astrophysical jet gas flows and shock wave patterns has been revealed in recent Hubble Space Telescope images. Simulating the imaged fluid flows and shock waves will help us understand the astrophysical processes at work in these jets.

We apply [Ha] the WENO-LF method—a modern high-order upwind method—to simulate high Mach number nonrelativistic astrophysical jets from young stars including the effects of radiative cooling. In the astrophysical setting, the jet gas is on the order of ten times the density of the ambient gas. Simulations at high Mach numbers and with radiative cooling are essential for achieving detailed agreement with the astrophysical observations. For example, the gas flows in the HH 1–2 astrophysical jets [Hester] are at about Mach 80. The WENO-LF method allows us to simulate astrophysical jets at much higher Mach numbers than have been attained (Mach 20) in the literature (see [Ha] and references therein). Note that the convention is to specify the Mach number of the jet with respect to the jet gas.

Computer simulations and astrophysical theory will allow us to analyze the detailed properties of the astrophysical flows including the shock waves that develop in and around the jet and the temperatures, densities, velocities, and chemical compositions of the jets. We are especially interested in how radiative cooling affects morphology and propagation of the jets.

Here we describe our implementation of the two-dimensional "slab" jet problem using the WENO-LF method, including a realistic model for radiative cooling. The simulations of the basic jet flows agree well with the Hubble Space Telescope images of HH 1–2. In addition, we present a preliminary model of the XZ Tauri proto-jet [Krist] including the pair of expanding bow shock "bubbles".

2. Gas Dynamics with Radiative Cooling

The equations of gas dynamics with radiative cooling take the form

$$\frac{\partial \rho}{\partial t} + \frac{\partial}{\partial x_i}(\rho u_i) = 0 \tag{1.1}$$

$$\frac{\partial}{\partial t}(\rho u_j) + \frac{\partial}{\partial x_i}(\rho u_i u_j) + \frac{\partial P}{\partial x_j} = 0 \tag{1.2}$$

$$\frac{\partial E}{\partial t} + \frac{\partial}{\partial x_i}(u_i(E+P)) = -n^2\Lambda(T) \tag{1.3}$$

where $\rho = m_H n$ is the density of the the gas (here assumed to be H), m_H is the mass of H, n is the number density, u_i is the velocity, ρu_i is the momentum density, $P = nk_BT$ is the pressure, k_B is Boltzmann's constant, T is the temperature, and

$$E = \frac{3}{2} nk_BT + \frac{1}{2}\rho u^2 \tag{1.4}$$

is the energy density. Indices $i,\ j$ equal 1, 2, 3, and repeated indices are summed over.

Radiative cooling of the gas is incorporated through the right-hand side of Eq. (1.3), with the model for $\Lambda(T)$ taken from Fig. 8 of [Schmutzler].

3. Numerical Methods

We use a third-order WENO [Shu] (weighted essentially non-oscillatory) method based on the scheme and gas dynamics code of Shu for our supersonic astrophysical flow simulations. We have extended and adapted [Ha] the code for simulating very high Mach number flows with radiative cooling.

ENO and WENO schemes are high-order finite difference schemes designed for nonlinear hyperbolic conservation laws with piecewise smooth solutions containing sharp discontinuities like shock waves and contacts. Locally smooth stencils are chosen via a nonlinear adaptive algorithm to avoid crossing discontinuities whenever possible in the interpolation procedure. The weighted ENO (WENO) schemes use a convex combination of all candidate stencils, rather than just one as in the original ENO method.

We now describe the computational procedure for the third-order WENO scheme in more detail. Spatial discretization is discussed first. We start with the simple case of a scalar equation

$$u_t + f(u)_x = 0 \tag{1.5}$$

and assume $\partial f(u)/\partial u \geq 0$, i.e., that the "wind direction" is positive. More general cases will be described later. A conservative numerical approximation $u_j(t)$ to the exact solution $u(x_j, t)$ of (1.5) satisfies the following ODE system:

$$\frac{du_j(t)}{dt} + \frac{1}{\Delta x}\left(\hat{f}_{j+1/2} - \hat{f}_{j-1/2}\right) = 0 \tag{1.6}$$

where $\hat{f}_{j+1/2}$ is called the numerical flux, the design of which is the key ingredient for a successful scheme. For the third-order WENO scheme,

the numerical flux $\hat{f}_{j+1/2}$ is defined as follows:

$$\hat{f}_{j+1/2} = \omega_1 \hat{f}^{(1)}_{j+1/2} + \omega_2 \hat{f}^{(2)}_{j+1/2} \tag{1.7}$$

where $\hat{f}^{(m)}_{j+1/2}$, for $m = 1, 2$, are the two second-order accurate fluxes on two different stencils given by

$$\hat{f}^{(1)}_{j+1/2} = -\frac{1}{2} f_{j-1} + \frac{3}{2} f_j, \quad \hat{f}^{(2)}_{j+1/2} = \frac{1}{2} f_j + \frac{1}{2} f_{j+1}. \tag{1.8}$$

The nonlinear weights ω_m are given by

$$\omega_m = \frac{\tilde{\omega}_m}{\sum_{l=1}^{2} \tilde{\omega}_l}, \quad \tilde{\omega}_l = \frac{\gamma_l}{(\varepsilon + \beta_l)^2} \tag{1.9}$$

with the linear weights γ_l given by

$$\gamma_1 = \frac{1}{3}, \quad \gamma_2 = \frac{2}{3} \tag{1.10}$$

and the smoothness indicators β_l by

$$\beta_1 = (f_j - f_{j-1})^2, \quad \beta_2 = (f_{j+1} - f_j)^2. \tag{1.11}$$

Finally, the parameter ε insures that the denominator in Eq. (1.9) never becomes 0, and is fixed at $\varepsilon = 10^{-6}$ in the computations presented here. The choice of ε does not affect accuracy: the numerical errors can be much lower than ε, approaching machine zero. Note that we have used the short-hand notation f_j to denote $f(u_j(t))$, and that the stencil for the scheme is biased to the left because of the positive wind direction.

The main reason that WENO works well, both for smooth solutions and for solutions containing shocks or other discontinuities or high gradient regions, is that the nonlinear weights, determined by the smoothness indicators, automatically adjust themselves based on the numerical solution to use the locally smoothest information given by the solution.

If the wind direction $\partial f(u)/\partial u \leq 0$, the method for computing the numerical flux $\hat{f}_{j+1/2}$ is the exact mirror image with respect to the point $x_{j+1/2}$ of the description above. The stencil would then be biased to the right. If $\partial f(u)/\partial u$ changes sign, we use a smooth flux splitting

$$f(u) = f^+(u) + f^-(u) \tag{1.12}$$

where $\partial f^+(u)/\partial u \geq 0$ and $\partial f^-(u)/\partial u \leq 0$, and apply the above procedure separately on each of them. There are many choices of such flux splittings; the most popular one is the Lax-Friedrichs flux splitting where

$$f^{\pm}(u) = \frac{1}{2} \left(f(u) \pm \alpha u \right) \tag{1.13}$$

with $\alpha = \max_u |\partial f(u)/\partial u|$.

For hyperbolic systems of conservation laws (1.5), the eigenvalues of the Jacobian $\partial f(u)/\partial u$ are all real, and there is a complete set of right and left eigenvectors. This allows us to apply the nonlinear WENO procedure in each of the local characteristic fields, obtained by using the left eigenvectors of the Jacobian. For multiple spatial dimensions, the finite difference version of WENO schemes simply applies the WENO procedure in each direction to obtain high order approximations to the relevant spatial derivatives. Unlike dimensional splitting, such a dimension by dimension method allows us to obtain high order accuracy without the computational cost of truly multidimensional reconstructions.

4. Astrophysical Jet Simulations

We first consider the fully developed jets in HH 1–2. Then we model the early stages of a jet—the XZ Tauri proto-jet.

jet	*ambient*
$\gamma = 5/3$	$\gamma = 5/3$
$\rho_j = 500$ H/cm^3	$\rho_a = 50$ H/cm^3
$u_j = 300$ km/s	$u_a = 0$
$T_j = 1000$ K	$T_a = 10{,}000$ K
$c_j = 3.8$ km/s	$c_a = 12$ km/s

Table 1.1. Parameters for the jets in HH 1–2.

The jets in HH 1–2 have the parameters listed in Table 2. The simulations were performed with the WENO-LF method on a $500\Delta x \times 250\Delta y$ grid. The jet width is 10^{10} km and the evolution time is 7×10^8 s ≈ 22 yr. The jet inflow is Mach 25 with respect to the soundspeed in the light ambient gas and Mach 80 with respect to the soundspeed in the heavy jet gas.

Our simulations with radiative cooling accurately reproduce the morphology and physics of the cylindrically symmetrical jet in HH 1–2, including the bow shock ahead of the jet, the terminal Mach disk just inside the tip of the jet, and the Kelvin-Helmholtz rollup of the jet tip. With radiative cooling, the jet has a much higher density contrast near the jet tip (as the shocked, heated gas cools radiatively, it compresses), a much thinner bow shock, reduced Kelvin-Helmholtz rollup of the jet tip, and a lower average temperature.

We also analyze the "turn-on" of the XZ Tauri proto-jet and its associated expanding pair of bow shock "bubbles".

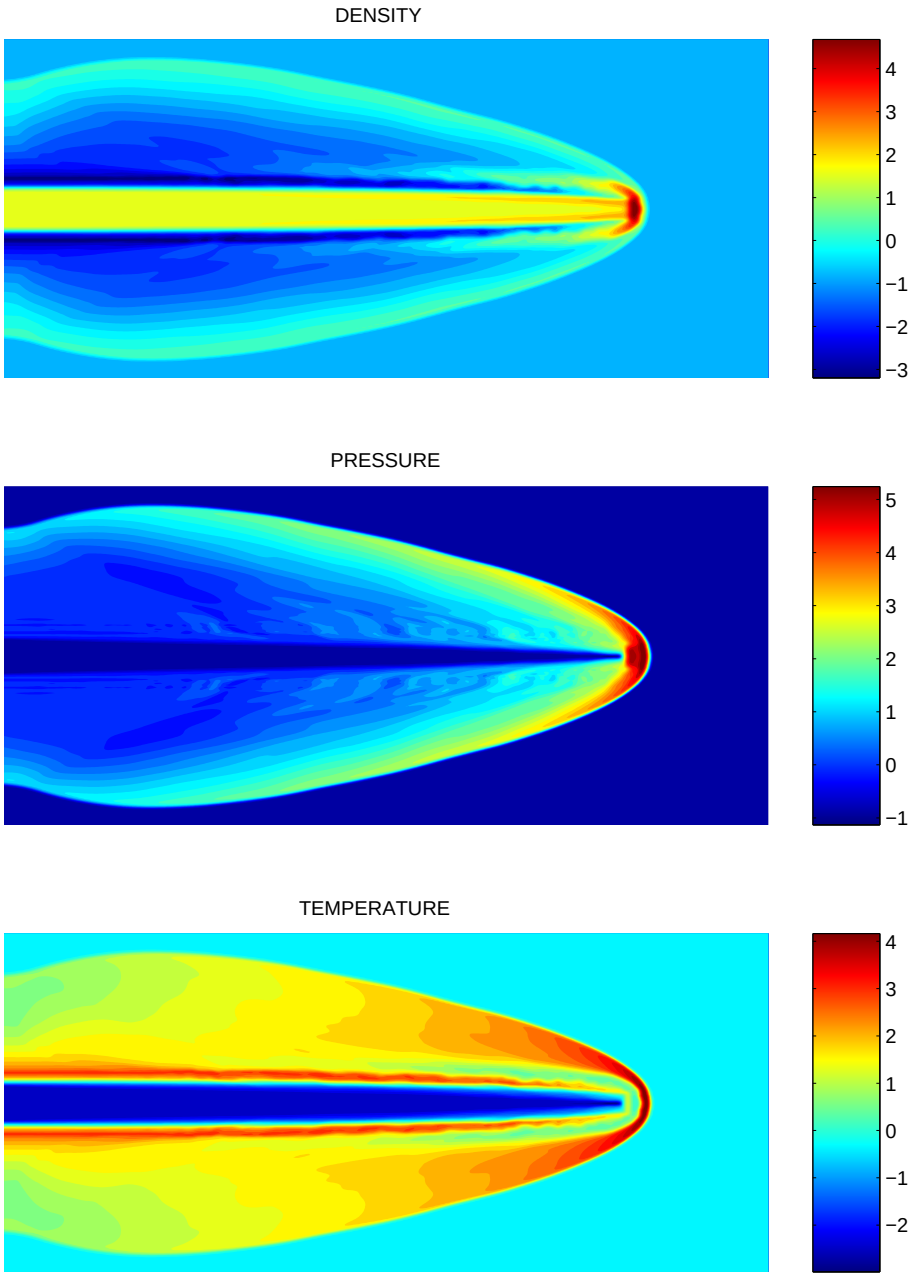

Figure 1.1. Simulation of Mach 80 jet with radiative cooling. Scales are logarithmic.

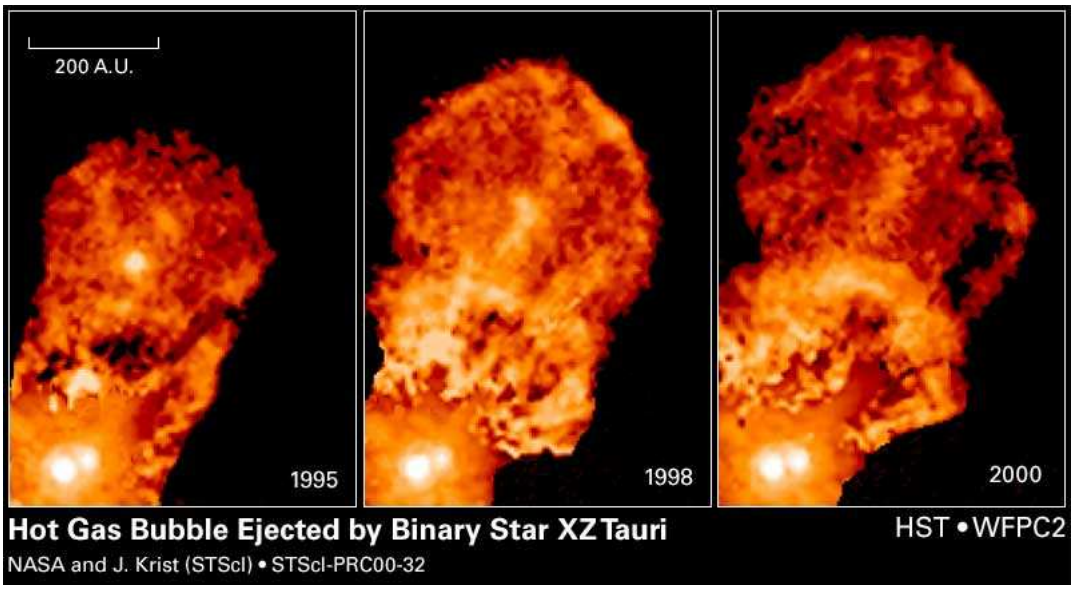

Figure 1.2. Evolution of XZ Tauri proto-jet.

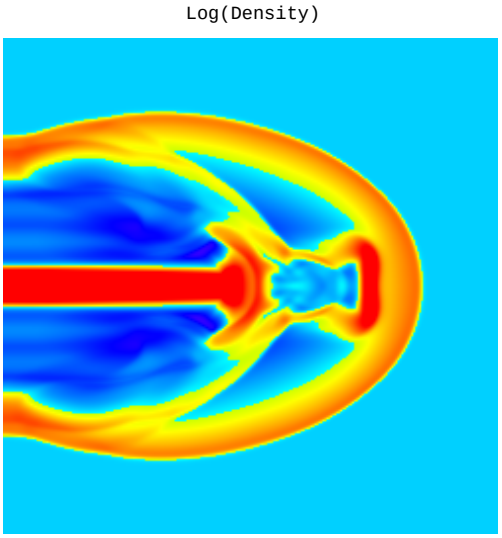

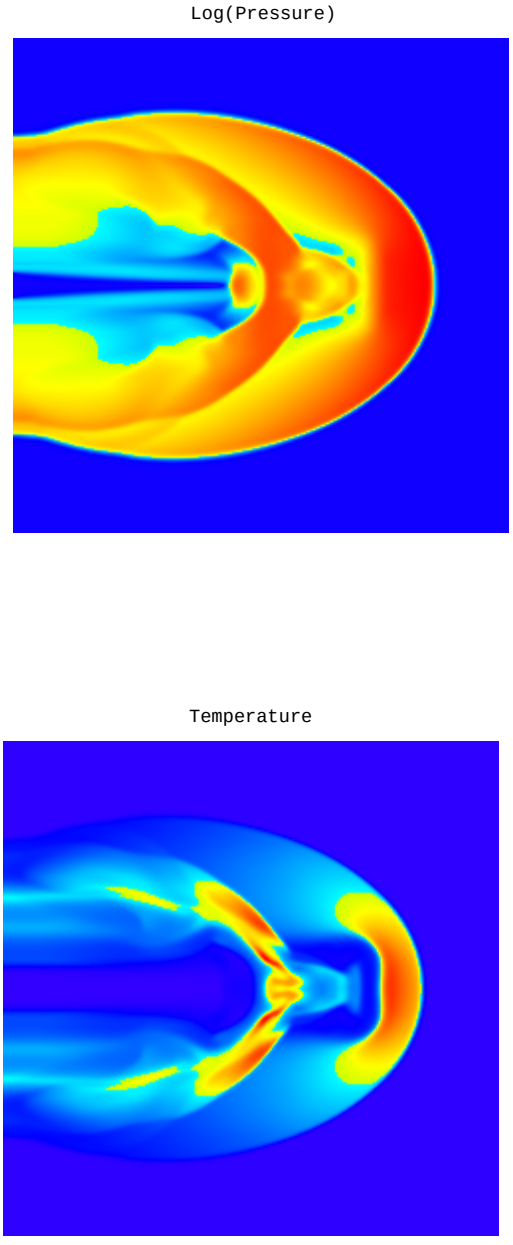

Figure 1.3. Numerical simulation of XZ Tauri jet.

We used the same parameters as for the HH 1–2 jets. The simulations were performed with the WENO-LF method on a $250\Delta x \times 250\Delta y$ grid. The jet width is 10^{10} km and the evolution time is 3.5×10^8 s ≈ 11 yr.

The Hubble images show a brightening (due to radiative cooling and compression of the gas) of the limb of the leading bow shock only at intermediate stages. If cooling is significant in the early stages, the simulated bow shocks are too thin to match the images, and the limb of the outer bow shock brightens too early. Thus in these preliminary simulations we have turned off radiative cooling. To obtain a realistic match with the astrophysical images, radiative cooling must be present but important only in the intermediate stages. This can be achieved by setting the parameters of the jet and ambient gas so that cooling is initially suppressed, but important later on as the bow shock advances.

We pulsed the jet outflow as follows: an initial jet pulse of 10^8 s, which is then turned off for 2×10^8 s, followed by a jet pulse of 4×10^8 s. The width of the simulated bow shocks does agree with the Hubble images: roughly 6×10^{10} km, so that the proto-jet plus bow shock "bubbles" can be modeled as a single outflow of a pulsed jet with two bow shocks. No extraneous wind is necessary to match the morphology of the imaged flows.

5. Conclusion

In order to make a detailed comparison of the simulations and the astrophysical images of the HH 1–2 and XZ Tauri jets, including reproducing the morphology, shock structure, and temperature/ionization profiles of the jets, we plan to extend the numerical code to a parallel version in three dimensions. Three-dimensional simulations with moderate resolution are feasible on modern workstations. The parallel version is needed to achieve high resolution of fully 3D flows and shock structures.

Acknowledgement

Research supported in part by the Space Telescope Science Institute under grant HST-GO-09863.06.

References

Y. Ha, C. L. Gardner, A. Gelb, and C.-W. Shu, "Numerical Simulation of High Mach Number Astrophysical Jets with Radiative Cooling," *Journal of Scientific Computing*, to appear.

J. J. Hester, K. R. Stapelfeldt, and P. A. Scowen, "Hubble Space Telescope Wide Field Planetary Camera 2 observations of HH 1–2," *Astronomical Journal* 116, 372–395, 1998.

J. E. Krist, K. R. Stapelfeldt, C. J. Burrows, J. J. Hester, A. M. Watson, G. E. Ballester, J. T. Clarke, D. Crisp, R. W. Evans, J. S. Gallagher, R. E. Griffiths, J. G. Hoessel, J. A. Holtzman, J. R. Mould, P. A. Scowen, and J. T. Trauger, "Hubble Space Telescope WFPC2 imaging of XZ Tauri: Time evolution of a Herbig-Haro bow shock," *Astrophysical Journal* 515: L35–L38, 1999.

T. Schmutzler and W. M. Tscharnuter, "Effective radiative cooling in optically thin plasmas," *Astronomy and Astrophysics* 273, 318–330, 1993.

C.-W. Shu, "High order ENO and WENO schemes for computational fluid dynamics," in *High-Order Methods for Computational Physics*, Lecture Notes in Computational Science and Engineering vol. 9, 439–582. New York: Springer Verlag, 1999.